Published in final edited form as:
Biomaterials. 2014 May ; 35(15): 4477–4488. doi:10.1016/j.biomaterials.2014.02.012.

The Role of Macrophage Phenotype in Vascularization of Tissue Engineering Scaffolds

Kara L. Spiller[1,2], **Rachel Anfang**[1], **Krista J. Spiller**[3], **Johnathan Ng**[1], **Kenneth R. Nakazawa**[1], **Jeffrey W. Daulton**[4], and **Gordana Vunjak-Novakovic**[1]

[1]Department of Biomedical Engineering, Columbia University, 622 West 168th Street, New York NY 10032

[2]School of Biomedical Engineering, Science, and Health Systems, Drexel University, 3141 Chestnut St., Philadelphia, PA 19104

[3]Department of Pathology, Columbia University, 630 west 168th Street, New York NY 10032

[4]Lincoln Laboratory, Massachusetts Institute of Technology, 244 Wood Street, Lexington, MA 02420

Abstract

Angiogenesis is crucial for the success of most tissue engineering strategies. The natural inflammatory response is a major regulator of vascularization, through the activity of different types of macrophages and the cytokines they secrete. Macrophages exist on a spectrum of diverse phenotypes, from “classically activated” M1 to “alternatively activated” M2 macrophages. M2 macrophages, including the subsets M2a and M2c, are typically considered to promote angiogenesis and tissue regeneration, while M1 macrophages are considered to be anti-angiogenic, although these classifications are controversial. Here we show that in contrast to this traditional paradigm, primary human M1 macrophages secrete the highest levels of potent angiogenic stimulators including VEGF; M2a macrophages secrete the highest levels of PDGF-BB, a

*Corresponding Author: Gordana Vunjak-Novakovic, PhD, Columbia University, 622 West 168th Street, VC12-234, New York, NY 10032, gv2131@columbia.edu.
Kara Spiller, Columbia University, Department of Biomedical Engineering, 622 west 168th Street, VC12-234, New York NY 10032, kspiller@coe.drexel.edu
Drexel University, School of Biomedical Engineering, Science, and Health Systems, 3141 Chestnut St., Philadelphia, PA 19104, kspiller@coe.drexel.edu
Rachel Anfang, Columbia University, Department of Biomedical Engineering, 622 west 168th Street, VC12-234, New York NY 10032, rachel.anfang@gmail.com
Krista Spiller, Columbia University, Department of Biomedical Engineering, 622 west 168th Street, VC12-234, New York NY 10032, kspiller1@gmail.com
Johnathan Ng, Columbia University, Department of Biomedical Engineering, 622 west 168th Street, VC12-234, New York NY 10032, jjn2113@columbia.edu
Kenneth Nakazawa, Columbia University, Department of Biomedical Engineering, 622 west 168th Street, VC12-234, New York NY 10032, krn2111@columbia.edu
Jefftrey W Dalton, MIT, Lincoln Laboratories, 244 Wood Street, Lexington, MA 02420, gv2131@columbia.edu
Gordana Vunjak-Novakovic, Columbia University, Department of Biomedical Engineering, 622 west 168th Street, VC12-234, New York NY 10032, gv2131@columbia.edu

chemoattractant stabilizing pericytes, and also promote anastomosis of sprouting endothelial cells *in vitro*; and M2c macrophages secrete the highest levels of MMP9, an important protease involved in vascular remodeling. In a murine subcutaneous implantation model, porous collagen scaffolds were surrounded by a fibrous capsule, coincident with high expression of M2 macrophage markers, while scaffolds coated with the bacterial lipopolysaccharide were degraded by inflammatory macrophages, and glutaraldehyde-crosslinked scaffolds were infiltrated by substantial numbers of blood vessels accompanied by high levels of M1 and M2 macrophages. These results suggest that coordinated efforts by both M1 and M2 macrophages are required for angiogenesis and scaffold vascularization, which may explain some of the controversy over which phenotype is the angiogenic phenotype.

Keywords

Macrophage; angiogenesis; inflammation; foreign body response; collagen

1. Introduction

The use of cell-instructive biomaterials to replace or regenerate damaged tissues is a core area of regenerative medicine. Early research focused largely on the chemical and mechanical properties of biomaterial scaffolds and considered the immune response a factor that needed to be minimized. Only recently, a notion is emerging that the inflammatory response can play a major role in integration and vascularization of biomaterial scaffolds [1]. Manipulation of the immune response could thus be beneficial to the design of future therapies. The goal of this study was to understand the specific role that the macrophage, the cell at the center of the inflammatory response, plays in vascularization of tissue engineering scaffolds.

Macrophages, originally believed to be solely pro-inflammatory and destructive phagocytes, were found in 1992 to have ability to convert to a pro-healing phenotype [2]. Since then, it has been shown that macrophages are necessary for angiogenesis, wound healing, tumor growth, and even limb regeneration in the salamander [3–6]. To distinguish this new phenotype from their familiar “classically activated” counterparts, these macrophages were referred to as “alternatively activated.” Since then, these “M2” macrophages, named following the helper T cell nomenclature (Th1/Th2) and in contrast to pro-inflammatory “M1” macrophages, have been associated with the resolution of wound healing *in vivo* in chronic leg ulcers [7], atherosclerotic lesions [8], traumatic spinal cord injury [9], and inflammatory renal disease [10, 11]. The role of tumor-associated macrophages, widely believed to belong to the class of M2 macrophages, in promoting angiogenesis is well-established [12]. However, the role of non-tumor-associated M2 macrophages in angiogenesis is poorly understood. While some studies showed that decreased ratios of the numbers of M1/M2 macrophages correlates with biomaterial vascularization [13–17], other studies showed that increased M1/M2 ratios correlates with more vascularization [18–20]. Also, the perceived anti-angiogenic behavior of M1 macrophages contradicts the fact that inflammatory diseases such as macular degeneration, psoriasis, atherosclerosis, diabetic

retinopathy, Crohn's disease, rheumatoid arthritis, and intervertebral disc degeneration are all characterized by excessive angiogenesis [21–26].

Understanding alternative activation of macrophages is further complicated by different subgroups within that classification. M2 macrophages were originally described as those stimulated with interleukin-4 (IL4), but the M2 designation was quickly expanded to include macrophages with very different characteristics [27]. The traditional M2 macrophages were called M2a, and macrophages stimulated with IL10 were called M2c. The difference between M2a and M2c macrophages, especially in the context of angiogenesis, remains unclear. Although it has been established that M1 macrophages appear at early stages of wound healing (1–3 days) and are later replaced with M2 macrophages (4–7 days) [28, 29], there is no clear distinction between M2a and M2c macrophages in this process.

Our objective was to better understand the distinctive roles of the M1 and M2 macrophage subtypes in angiogenesis and vascularization of biomaterials, and to devise strategies for designing scaffolds that can effectively induce and mediate vasculogenesis. To this end, we analyzed gene expression and protein secretion profiles in M0, M1, M2a, and M2c macrophages for angiogenesis *in vitro*, and then investigated the *in vivo* vascularization of scaffolds selected to elicit specific macrophage responses.

2. Materials and methods

2.1. Monocyte isolation and preparation of polarized macrophages and conditioned media

Monocytes were isolated from buffy coats (obtained from the New York Blood Center) using sequential density gradient centrifugations of Ficoll and Percoll 46% [30]. The yield of CD14+ monocytes, assessed by flow cytometry, was typically around 70%. The monocytes were cultured in ultra low attachment flasks in RPMI 1640 medium with 10% heat-inactivated human serum and 20ng/ml monocyte colony stimulating factor (MCSF) to differentiate them into macrophages. Tissue culture polystyrene has been shown to promote activation of monocytes and macrophages compared to Teflon-coated surfaces [31], and we found in preliminary studies that ultra low attachment plastic produced similar yet more consistent results compared to Teflon. The media was changed at day 3, and by day 5, the macrophages were attached to the plastic. Polarization was begun by changing to fresh media supplemented with 20ng/ml MCSF and the following cytokines: 100ng/mL interferon-gamma (IFN$\boldsymbol{\gamma}$) and 100ng/mL lipopolysaccharide (LPS) for M1; 40ng/mL IL4 and 20ng/mL IL13 for M2a; and 40ng/mL IL10 for M2c. After 48 hours of polarization, macrophages were collected by gentle scraping. A small sample was taken for gene expression analysis, and the rest of the cells were incubated in fresh medium at 10^6 cells/mL with no cytokines for 24 hours. Macrophages were collected by scraping and analyzed by flow cytometry, and the conditioned media was centrifuged at 400g for 10min and frozen at −80°C until analysis or use for culture of endothelial cells.

2.2. LPS contamination

Medium was tested for LPS contamination using the Pierce LAL Chromogenic Endotoxin Quantification kit according to manufacture's instructions. LPS contamination was always < 0.2 EU/mL.

2.3. Flow cytometric analysis

The expression of surface antigens was evaluated by incubating 125,000 M0, M1, M2a or M2c macrophages at 4°C for 1 hour with the respective antibodies in 100μL FACS buffer (1mM EDTA in PBS with 0.5% BSA) (Sigma). The molecules evaluated were the antigen-presenting molecule HLA-DR, chemokine receptor CCR7, scavenger receptor CD163 and the mannose receptor CD206. The following antibodies were used for evaluation: FITC-conjugated mouse antibodies against CD206 (Biolegend.com, catalog no. 321103, dilution 1:100), APC-conjugated mouse antibodies against CD163 (Abcam, catalog no. ab134416, dilution 1:50) and CCR7 (Biolegend.com, catalog no. 353213, dilution 1:50), and PE-conjugated mouse antibodies against HLA-DR (Abcam, catalog no. ab113839, dilution 1:100). Corresponding isotype controls were used as recommended by the manufacturers for comparison with each antibody. Labeled cells were washed twice in 1mL FACS buffer and fixed using Cytofix (BD Pharminogen). The samples were analyzed using a FACSCalibur flow cytometer and the CellQuest software (BD Biosciences, Pharminogen). Data was processed using FlowJo (Tree Star) and the percentage population of each cell type that stained positively for the respective markers was compared by gating at 1% inclusion of isotype controls to eliminate non-specific staining.

2.4. RNA extraction and cDNA synthesis

RNAqueous®-Micro kit (Life Technologies) for RNA extraction was used according to the manufacturer's instructions, eluting the samples at the final step with 5μL of elution solutions three times. The quantity of RNA was measured on a Nanodrop ND1000 and considered pure if the ratio of absorbance at 260nm/280nm was ≥ 2. The samples were then stored at −80°C until used for reverse transcription. The RNA was first treated with DNase I removal kit (Invitrogen) according to the manufacturer's instructions. cDNA synthesis was preformed using High Capacity kit from Applied Biosystems according to the manufacturer's instructions. Each reaction tube contained ≤ 1000ng RNA.

2.5. Quantitative analysis of gene expression using RT-PCR

Quantitative RT–PCR analysis was performed using 20ng cDNA per reaction and the SYBR® Green PCR Master Mix (Applied Biosystems by Life Technologies). The expression of target genes was normalized to the housekeeping gene *GAPDH*, and then to the unactivated M0 phenotype ($2^{-\Delta\Delta Ct}$). Gene expression values were calculated by using the mean C_T values of the samples. All primers (Table S1) were synthesized by Life Technologies.

2.6. Secreted protein quantification using ELISA

Human VEGF and PDGF-BB Mini ELISA Development Kits (Peprotech) and MMP9 Quantikine ELISA kits (R&D Systems) were used according to the manufacturer's instructions.

2.7. Gel zymography

Conditioned media was assessed for enzymatically active MMP9 content using gel zymography (Novex Zymogram gels, Life Technologies). 5μL of conditioned medium was

loaded into the 10% Zymogram (gelatin) gel and run for 90 min at 120V. The gel was developed overnight and stained with SimplyBlue.

2.8. Endothelial cell isolation and culture

Human umbilical cord derived endothelial cells (HUVECs) were isolated from fresh umbilical veins from the neonatal unit at Columbia University following an approved IRB protocol (IRBAAAC4839) according to previously described methods [32]. HUVECs were cultured in endothelial growth media (EGM-2, Lonza) and cells from passage 2–4 were used in experiments.

2.9. *In vitro* sprout formation analysis

Transparent hanging transwell inserts (Millipore, 0.4μm pore size) were coated in 40μL of a 1:1 solution of Matrigel® and endothelial basal media (EBM2) and incubated for 1 hour at 37°C. Each insert was placed in a 24-well plate containing 400μL of macrophage-conditioned media with an additional 100μL added directly into each insert (n = 3–5 replicates per phenotype per donor, n=3 donors). RPMI media with 10% heat inactivated human serum and EGM2 were used as negative and positive controls, respectively. 20,000 HUVECs were added to each insert and were cultured at 37°C for 18 hours. The cells were then stained with a Live/Dead® kit (Invitrogen) following the manufacturer's instructions and the networks were imaged with the 10x objective of an Olympus IX81 microscope. Calcein-AM was used to indicate live cells, and ethidium homodimer-1 was used to indicate dead cells. Two or three images of each sample were required to capture all sprouts in the samples. Background was removed and the networks were analyzed as described in Fig. S1. Briefly, the images were stitched together using the pairwise and grid/collection stitching toolbox in FIJI [33] resulting in one image per sample. The fused images were converted into 8-bit TIFF files and adjusted for brightness/contrast to distinguish the networks against the background. A custom-designed algorithm in MATLAB was utilized to remove any noise (*i.e.* structures not part of the network). Functions from the Image Processing Toolbox in MATLAB were employed to perform the image manipulation. A map of the background was generated and subtracted from the image, resulting in an image with a completely dark field that was converted into a set of binary images with varying gray threshold values. Morphological cleaning, bridging, and closing operations were performed on images to smooth the edges of the network and maintain connectivity over fine structural elements. The resulting set of images contained the network elements at varying threshold values, allowing for the creation of a single binary image with each element incorporated at an optimal gray threshold. An element-by-element multiplication was performed between this binary image and the original microscope image to yield a final clean image for network analysis. For each sample, the total area of the networks was calculated in MATLAB and the number of sprouts and nodes was determined using the Angiogenesis Analyzer macro in ImageJ [34]. To determine the number of sprouts, the Analyzer was set to resolve the number of segments, isolated segments, and branched segments. To determine the number of nodes, the Analyzer was set to locate each junction point.

2.10. Viability and metabolic assays

HUVECs were starved overnight in EBM2 with 0.5% fetal bovine serum (FBS) prior to seeding at a density of 5,000 cells per well in 100μl conditioned media in a 96-well plate (n=9 per group). EGM-2 was used as a positive control and RPMI with 0.5% FBS was used as a negative control. After 18 hours, the wells were washed with PBS and DNA content was quantified using Quant-iT™ PicoGreen® dsDNA Assay kit (Invitrogen) according to the manufacturer's instructions. DNA was quantified using a standard curve prepared using λ-phage DNA. Metabolic activity of the cells during the viability study was measured using Alamar Blue® reagent according to the manufacturer's instructions (Life Technologies).

2.11. *In vitro* fibrin assay

Fibrinogen (4mg/ml) was mixed in equal parts with thrombin (0.2 U/ml), and 100μl was added to each well of an 8-well chamberslide (Thermo Scientific Nunc Labtek). Gelation was allowed to occur for one hour at 37°C, and then 8,000 HUVECs were added to each well in 200μl EGM-2 overnight. Media was changed to 300μl conditioned media from M0, M1, M2a, or M2c phenotypes, or a 33/33/33 combination of M1, M2a, and M2c phenotypes. Basal media (RPMI with 10% heat-inactivated human serum) was used as a control. After 24 hours in macrophage-conditioned media, the media was changed again to either media conditioned by the same phenotype of macrophages, or different macrophages, in order to evaluate sequential application of different signals. After 3 days (4 total days of culture in macrophage-conditioned media), the samples were washed and fixed with 4% paraformaldehyde directly in the chamberslides. The samples were stained with DAPI to visualize cell nuclei and Alexafluor-488 Phalloidin (Life Technologies) to visualize actin filaments, and imaged using an Olympus Fluoview FV1000 Confocal microscope.

2.12. Scaffold preparation and subcutaneous implantation

Cylindrical disks (7mm in diameter × 2.5mm thick) were punched from sheets of collagen sponge (Avitene™ Ultrafoam™). Scaffolds were either soaked in PBS ("Collagen"), 0.1% glutaraldehyde in PBS ("Glutaraldehyde-crosslinked"), or 100ng/ml LPS ("LPS-coated") for 4 hr. Then, scaffolds were washed 4 times for 10 min in PBS, and incubated in RPMI medium for 4 days. Glutaraldehyde-crosslinked scaffolds were incubated for 4 hr in 0.1M glycine to quench any residual glutaraldehyde and then in RPMI medium overnight.

All animal experiments followed federal guidelines and were conducted under a protocol approved by the Columbia University Animal Care and Use Committee. Scaffolds from the above three groups were implanted subcutaneously in male 8-week-old C57BL/6 mice for 10 days (one sample per mouse, n=3 mice per group). In addition, to eliminate the effects of animal-to-animal differences, one scaffold of the unmodified collagen and one glutaraldehyde-crosslinked scaffolds were implanted into three mice (n=6). Mice were anesthetized using 100mg/kg ketamine and 10mg/kg xylazine and shaved. A small incision (<1cm) was made using a scalpel in the central dorsal surface. Blunt forceps were used to create a pocket in the subcutaneous space for the scaffolds. After implantation, wounds were closed with two sutures. Mice were monitored and housed for 10 days. No signs of discomfort were observed following surgery throughout the study.

2.13. Explant and histological analysis

After 10 days, mice were euthanized by CO_2 asphyxiation. An incision was made and the skin was pulled back to expose the scaffolds. Gross view images were taken immediately with an Olympus SZX16 stereomicroscope. The scaffolds and surrounding tissue were excised and fixed in 4% paraformaldehyde overnight. The samples were washed for 6 hours in PBS, incubated in 30% sucrose for 3 days, embedded in OCT (Tissue-Tek, Torrance, TA) and frozen. Samples were sectioned to 5μm and mounted onto slides for histological evaluation. Tissue structure was examined by staining with hematoxylin and eosin (H&E), which stains nuclei dark blue to black, and cytoplasm and collagen pink. Images of whole tissue sections were obtained using the stitching function of an Olympus FX100 microscope and software.

2.14. Immunofluorescence

Sections were analyzed for three markers of the M1 phenotype (TNF-alpha, iNOS, and CCR7) and three markers of the M2 phenotype (CD206, Arg1, and CD163), along with the pan-macrophage marker F480, using the antibodies and dilutions described in [16] and CD163 (1:50) from Santa Cruz Biotechnology. Endothelial cells were stained with rabbit-anti-mouse CD31 (1:50) from Abcam.

2.15. Statistical analysis

Data are shown as Mean ± SEM. Statistical analysis was performed in GraphPad Prism 5.0 using one-way ANOVA with post-hoc Bonferroni analysis. $P<0.05$ was considered significant.

3. Results

3.1. Characterization of polarized macrophages

Monocytes isolated from peripheral human blood were differentiated to macrophages through the addition of MCSF, and polarized to different macrophage phenotypes via the addition of specific cytokines (Fig. 1a). Three macrophage phenotypes were prepared (M1, M2a, M2c) and compared to an unactivated control phenotype (M0).

Gene expression analysis revealed that each macrophage phenotype uniquely upregulated specific markers. M1 macrophages strongly upregulated the inflammatory proteins interleukin-1-beta (*IL1b)* and tumor necrosis factor-alpha (*TNFa*) and the surface markers *CCR7*, *CD80*, and *HLA-DR*/*MHC Class II* (Fig. 1b). M2a macrophages upregulated the cytokines *CCL18* and *CCL22* and the surface marker *MRC1/CD206*. M2c macrophages could be distinguished by expression of the scavenger receptor *CD163*. Interestingly, M2c macrophages, typically considered anti-inflammatory, expressed higher levels of the inflammatory markers *TNFa* and *HLA-DR* than M2a. These levels were lower but not statistically different from M1 macrophages. CD163+ macrophages have been shown in other reports to secrete inflammatory cytokines in response to biomaterials *in vitro* [35] and in skin of psoriatic patients [23].

Flow cytometric analysis was used to confirm that the above surface markers are robust indicators of the macrophage phenotypes. CCR7 was expressed more strongly by M1 macrophages, although expression was still detected in the other phenotypes (Fig. 2a). Similarly, CD163 was expressed in the M2c phenotype, and M0 macrophages expressed similar levels. Surprisingly, the putative M2a marker CD206 and the M1 marker HLADR were expressed in almost all macrophage phenotypes (Fig. 2a). Moreover, a large fraction of CCR7+ cells of each phenotype was also positive for CD206, and all CD163 positive cells were positive for CD206 (Fig. S2a), indicating that the mere expression of these markers should not be used as definitive evidence of macrophage phenotype. It should be noted that transcriptional profiling has shown that MCSF-dependent differentiation of monocytes to macrophages is associated with upregulation of a significant number of M2a-associated genes, suggesting that their “default” state under homeostatic conditions might be slightly skewed to the M2a phenotype [36]. However, the mean fluorescent intensity per cell, an indication of how strongly each individual cell expressed the marker, revealed significant differences between the phenotypes (Fig. 2b and Fig. S2b). Thus, expression above a certain threshold of fluorescence may be useful as a phenotype marker.

3.2. Secretion of proteins related to different stages of angiogenesis

We next analyzed the expression of genes and secretion of proteins involved in angiogenesis (Fig. 3a). M1 macrophages expressed genes involved in the initiation of angiogenesis, including those that are chemotactic for endothelial cells: *VEGF*, basic fibroblast growth factor (*FGF2*), *IL8*, and *CCL5/RANTES* [37–41]. Secretion of VEGF was also confirmed on the protein level (Fig. 3b). The inflammatory cytokines TNF-alpha and IL1-beta, secreted by M1 macrophages [42], have been shown to prime endothelial cells for sprouting by promoting the tip cell phenotype [43] and to stimulate endothelial cells to recruit supporting pericytes [44]. Taken together, these results suggest that M1 macrophages are important initiators of angiogenesis.

M2a macrophages expressed and secreted high levels of PDGF-BB (Fig. 3a, 3b), a factor known to recruit pericytes [45, 46] and mesenchymal stem cells [47], which in turn stabilize the forming vasculature. Without this action, VEGF-stimulated blood vessels are leaky, immature, and prone to regression [48, 49]. M1 macrophages also expressed high levels of heparin binding EGF-like growth factor (*HBEGF*) (Fig. 3a), suggesting that they can also recruit pericytes. Interestingly, M2a macrophages expressed high levels of tissue inhibitor of matrix metalloprotease-3 (TIMP3) (Fig. 3a), which inhibits not only the enzymatic activity of MMP9 but also VEGF signaling, by blocking its binding to VEGF receptor 2 to result in potent inhibition of angiogenesis [50]. TIMP3 also blocks the release of TNF-alpha [51]. Therefore, M2a macrophages may help support angiogenesis by recruiting pericytes and regulating the signaling of M1 macrophages.

MMP9 is a potent stimulator of angiogenesis *in vitro* and *in vivo*, contributing to remodeling of the extracellular matrix in order to allow endothelial cells to migrate, among other functions [52, 53]. High levels of MMP9 were secreted by all groups, with M2a macrophages secreting significantly less MMP9 than the other phenotypes (Fig. 3b). The MMP9 was confirmed to be enzymatically active by gel zymography (Fig. 3c).

3.3. Effects of macrophage-conditioned media on angiogenesis *in vitro*

To assess the functional role of macrophage-secreted factors in angiogenesis, an *in vitro* sprouting assay was performed. HUVECs organized into networks with significantly more sprouts and greater total length in M2c-conditioned media compared to HUVECs in media conditioned by M1 or M2a macrophages (Fig. 4a). Interestingly, conditioned media from M0 macrophages also increased sprouting. The trends in sprouting mirror the secretion profiles of MMP9 (Fig. 3b), which is produced at high levels by macrophages and has previously been described to induce endothelial sprouting *in vitro* [52]. MMP9 has also been shown to promote neovascularization *in vivo*, partly by proteolytic release of sequestered VEGF [54]. Future studies are required to confirm if macrophage-mediated regulation is dose-responsive with MMP9.

Contrary to the traditional “angiogenic” role of M2a macrophages, endothelial cells in M2a-conditioned medium produced the shortest networks with the least number of sprouts, values that were not statistically different than the baseline media of RPMI with 10% heat inactivated human serum (Fig. 4a). No differences in viability or metabolic activity of HUVECs were found during the experimental time frame (Fig. S3), indicating that cell death was not the reason for the lack of sprouting in M2a-conditioned media.

To characterize the effects of changing dynamic signaling from macrophages on angiogenesis in a longer-term assay, endothelial cells were cultured on fibrin gels over 4 days in macrophage-conditioned media. The organization of endothelial cells in media conditioned by a single macrophage phenotype was compared to that of endothelial cells cultured in media that was switched after 24 hours from one macrophage phenotype to another. Endothelial cells organized into loosely interconnected clusters in M1-conditioned media, but not in media conditioned by the other phenotypes or a combination of all three (Fig. 5; higher magnification images in Fig. S4). When the media was switched at 24 hours from M1- to M2a-conditioned media, simulating the natural transition observed *in vivo* [28], the networking behavior was clearly enhanced, although we did not quantify these changes. Interestingly, this behavior was not observed when endothelial cells were cultured in M1 media followed by M2c or basal media, but it was observed when M2a media followed basal media. Thus, M2a macrophages secrete some signals that that cause fusion of sprouting vessels, but only if the signals are removed for a certain period of time, because endothelial cells did not form networks when cultured continuously in M2a media. These data are consistent with recent work showing that macrophages guide fusion of sprouting blood vessels in developmental angiogenesis *in vivo*, ensuring successful completion of angiogenesis [55, 56]. The previously observed close physical association of macrophages and fusing endothelial cells in these studies, in combination with the critical role of Notch signaling [56], suggested that cell-cell contact was required. In contrast, our study revealed similar effects of cell-secreted factors present in culture media.

Although traditional markers of the M1 and M2 phenotype were not assessed in the aforementioned studies of sprout-fusing macrophages, they were noted to be antigenically distinct from inflammatory macrophages [55]. In addition, blood vessel sprouting was induced by VEGF, while macrophage-mediated anastomosis did not involve VEGF. In light

of our results, in which M2a macrophages promoted anastomosis without secreting VEGF, it is tempting to speculate that the macrophages in those studies were of the M2a phenotype.

3.4. Role of macrophage phenotype in vascularization of tissue engineering scaffolds *in vivo*

To confirm the roles of macrophage phenotype for vascularization of biomaterials *in vivo*, collagen scaffolds designed to elicit a range of macrophage phenotypes were implanted subcutaneously in mice for 10 days. Glutaraldehyde-crosslinked scaffolds were expected to promote a moderate inflammatory response [13, 57]. Scaffolds soaked in LPS, a component of the bacterial cell wall that is frequently used to polarize macrophages to the M1 phenotype, were expected to elicit a strong M1 response. Unmodified collagen scaffolds served as a control.

There were marked differences in the inflammatory responses to the three scaffold groups after 10 days of implantation. A dense fibrous capsule surrounded unmodified collagen scaffolds (Fig. 6a and 6b), which has been previously described [58]. No blood vessels were observed in histological sections, and no staining by the endothelial cell marker CD31 could be detected (Fig. 6c). In contrast, glutaraldehyde-crosslinked scaffolds were well vascularized, with visible blood vessel infiltration both macroscopically (Fig. 6a) and in histological sections (Fig. 6b), where the latter showed abundant staining by CD31 (Fig. 6c). LPS-coated scaffolds were completely infiltrated by large numbers of inflammatory cells (Fig. 6b) with no evidence of blood vessels (Fig. 6c). Both control and LPS-coated scaffolds were considerably smaller and more degraded than the crosslinked scaffolds (Fig. 6a), consistent with the notion that crosslinking prevents degradation [59].

To identify the macrophage subtypes involved in different inflammatory responses, sections were stained for multiple markers of macrophage phenotype (Fig. 7a–d). Given that differences between murine M2a and M2c macrophages have not been systematically characterized, we did not attempt to differentiate between these. Instead, we used traditional M1 and M2 markers in combination with the pan-macrophage marker F480 to describe the phenotypes surrounding the scaffolds.

Both glutaraldehyde-crosslinked and LPS-coated scaffolds were infiltrated by F480+ macrophages, while macrophages remained primarily in the fibrous capsule surrounding the unmodified collagen scaffolds (Fig. 7). Due to the high levels of autofluorescence in the glutaraldehyde-crosslinked samples (Fig. 7e), the large numbers of macrophages surrounding the scaffolds, and the fact that positive staining does not necessarily indicate phenotype (Fig. 2a), it was not possible to quantify individual macrophage phenotypes, and the qualitative observations are summarized in Table 1. As expected, macrophages surrounding collagen scaffolds stained weakly for the M1 markers TNF-alpha and iNOS and strongly for the M2 markers CD206, Arg1, and CD163. Expression of Arg1 was notably higher in macrophages surrounding unmodified collagen scaffolds than in the other scaffolds. The vascularized glutaraldehyde-crosslinked scaffolds stained strongly for all M1 and M2 markers examined except for Arg1. LPS-coated scaffolds stained strongly for the M1 markers TNF-alpha, iNOS, and CCR7, and weakly for the M2 markers Arg1 and CD163. There were no apparent differences in CD206 or CCR7 expression among the

groups. The observed contributions of both M1 and M2 macrophages to angiogenesis *in vivo* corroborate the *in vitro* findings and further support the necessity of mobilizing diverse macrophage responses for achieving robust vascularization.

Discussion

The roles of various macrophage populations in angiogenesis are controversial and poorly understood [60]. Despite considerable evidence to the contrary [61], M1 macrophages are often considered “anti-angiogenic” [62], and the pro-fibrotic behavior of M2 macrophages [63–65] is ignored. Given the increasing biological complexity and immunomodulatory potential of biomaterials [66], it is essential to understand which macrophages are beneficial to vascularization and healing. Macrophages have been recognized as crucial regulators of healing for a long time [67], as their depletion causes drastically reduced angiogenesis and healing [55, 68–72], while exogenous addition of macrophages causes increased angiogenesis [73, 74]. In one study, vascularization of polymeric scaffolds was entirely dependent on the action of recruited macrophages, and was increased by incorporating monocyte chemoattractant protein-1 (MCP-1) [1]. Tissue engineering strategies that exert control over macrophages would be highly desired as they utilize the body’s own healing response to naturally promote regeneration.

Blood vessel networks grow through a process of sprouting, anastomosis, and maturation [75]. In response to angiogenic factors like VEGF, endothelial cells differentiate into tip cells and stalk cells, which lead and support sprouting vessels, respectively. The action of proteases like MMP9 is critical for the sprouting process. Newly sprouted vessels fuse with other vessels in anastomosis, and supporting pericytes are recruited via PDGF-BB to stabilize and develop the sprouts into mature vessels.

We show that the macrophages of all three activated phenotypes investigated in this study have the potential to contribute to angiogenesis. M1 macrophages secreted factors that are well-described to initiate the process of angiogenesis, including VEGF; M2a macrophages secreted factors known to be involved at later stages, especially PDGF-BB; and M2c macrophages promoted sprouting *in vitro* and secreted high levels of MMP9, suggesting a role in remodeling. Interestingly, factors secreted by M1 and M2c macrophages promoted sprouting of endothelial cells in the short-term Matrigel assay, while M2a signaling promoted network formation in the longer-term fibrin assay, but only if the signals were first removed for a period of time. M1-secreted factors TNF-alpha, IL1-beta, and VEGF have each been shown to promote blood vessel sprouting by inducing an endothelial tip cell phenotype [43, 55], while signaling from M2a macrophages promoted anastomosis (Fig. 5). Macrophage-mediated anastomosis has been shown to involve Notch1 signaling [56], but the secreted factors remain unknown. These results, in combination with the fact that continued presence of M1 and M2 macrophages resulted in neovascularization of scaffolds *in vivo*, suggest that coordinated involvement of both subsets of macrophages guides new vessel formation (Fig. 8). We propose a model in which M1 macrophages promote sprouting of blood vessels via secretion of VEGF, bFGF, IL8, RANTES, and TNF-alpha; M2c macrophages also support angiogenesis, probably by increasing vascular remodeling given their high levels of production of MMP9; and M2a macrophages promote fusion of blood

vessels through currently unidentified secreted factors. M2a macrophages may also regulate the actions of M1 macrophages via production of TIMP3, and may recruit pericytes via secretion of PDGF-BB, although these actions were not directly assessed in this study. The interplay between M1 and M2 macrophages in regulating angiogenesis, and particularly the effects of timing, deserves significantly more attention.

While macrophages clearly direct endothelial cell behavior, crosstalk in the other direction has also been described recently. Co-culture with endothelial cells caused macrophages to exhibit M2 polarization, which was partially mediated by VEGF [76, 77]. In a porcine model of renal injury, infusion of endothelial outgrowth cells decreased the ratio of M1/M2 macrophages at the site of injury [77]. Infusion of VEGF had a similar effect on the macrophages [77]. From these studies it appears that endothelial cells appear to provide a "vascular niche" [78] that may facilitate the M1-to-M2 transition, which is required for proper resolution of wound healing. Thus, continued crosstalk between macrophages and endothelial cells guides vascularization.

In the present study, complete scaffold vascularization was achieved by modifying scaffold properties in order to modulate the inflammatory response. Both M1 and M2 macrophages were required to achieve vascularization; scaffolds with a primarily M2 response were surrounded by a fibrous capsule, and those with a primarily M1 response were characterized by infiltrating inflammatory cells. The present study and others [18–20] showed that M1 macrophages are beneficial for scaffold vascularization *in vivo*. These results may appear contradictory to those that found increased vascularization of biomaterials with increased numbers of M2 macrophages [13–17]. However, in all of these studies, high numbers of M1 macrophages were also present. In fact, the authors of these studies noted that mixed phenotypes were coincident with vascularization [79].

Collagen scaffolds were chosen as a model biomaterial to examine the role of macrophage phenotype in vascularization for tissue engineering. Unmodified collagen scaffolds have been previously reported to provoke fibrous encapsulation [58], while crosslinking with glutaraldehyde caused both increased inflammation and vascularization in subcutaneous implantation [57]. The greater levels of M2 marker expression surrounding unmodified collagen scaffolds suggest involvement in fibrous capsule formation, which has been described elsewhere. For example, when macrophages are forced to the M2a phenotype *in vitro* through the addition of IL4, they fuse into foreign body giant cells, precursors to the fibrous capsule [80]. IL4 has long been known to be required for fibrous capsule formation *in vivo* [81], which decreases upon inhibition of the M2 marker CD206 [82]. On the other hand, persistence of M1 macrophages without M2 macrophages results in chronic inflammation and impaired resolution of healing in numerous situations [8–11]. Taken together, the collective data from the present study suggest that (a) *both* M1 and M2 macrophages are required for scaffold vascularization, and (b) if the balance of macrophage phenotype is pushed far enough towards either M1 or M2, then vascularization and integration cannot be achieved.

The results of this study highlight the complexity of macrophage control over angiogenesis, and several future studies are required to fully describe this system. While several studies

have profiled the differences in gene expression between M1 and M2a macrophages [36], very few have quantified the amount of secreted proteins, the most relevant outcome of polarization, and few studies have addressed the M2c phenotype at all [10, 83, 84]. Most importantly, the kinetics of macrophage-endothelial cell interactions in angiogenesis must be elucidated. It is well known that sequential release of VEGF and PDGF-BB from biomaterial scaffolds increases angiogenesis *in vivo* [85], suggesting that sequential activation of M1 and M2a macrophages, which secrete these two factors, would be beneficial. However, in this study, high numbers of M1 macrophages were present in vascularized scaffolds after ten days of subcutaneous implantation, suggesting a role for M1 macrophages at later times after injury. Studies are underway to investigate these temporal aspects of macrophage polarization.

There were some limitations to this study. Most notably, the subcutaneous implantation model is not necessarily clinically relevant, and it is possible that the response of macrophages at other sites of implantation may be different, especially in highly vascular areas such as bone, avascular areas such as cartilage, or load-bearing tissues such as tendon. In addition, the C57BL/6 strain is a commonly used animal model for biomaterial evaluation, but macrophage behavior is likely to be different in other strains of mice or animal models, and especially in humans [86]. Moreover, patient comorbidities associated with inflammation would almost certainly affect the macrophage response to implanted biomaterials. Another significant limitation of the study is that macrophage phenotype could not be quantified in histological sections due to the substantial autofluorescence of glutaraldehyde. Future studies should employ flow cytometry on digested tissue to quantify polarized macrophage populations. Finally, given the complexity of macrophage responses to biomaterials, which depend on material chemistry, mechanical properties, degradation, etc. [66], caution should be exercised in generalizing the results of macrophage response to the scaffolds studied in the present work to that of other biomaterials. For example, glutaraldehyde crosslinking and adsorption of LPS were chosen in order to elicit a moderate and strong M1 response, respectively, but are also likely to have diverse downstream effects.

Conclusions

We have systematically characterized three activated macrophage phenotypes (M1, M2a, and M2c) in the context of angiogenesis and vascularization of tissue engineering scaffolds and found evidence that all three phenotypes support angiogenesis in different ways. M1 and M2c macrophages induced endothelial cell sprouting, while M2a macrophages promoted anastomosis. By modifying scaffold properties to control the macrophage response, we were able to achieve robust scaffold vascularization. Tissue engineering strategies that incorporate knowledge of macrophage behavior may result in control over vascularization and integration, which is critically important for the clinical translation of all tissue-engineering strategies.

Supplementary Material

Refer to Web version on PubMed Central for supplementary material.

Acknowledgments

The authors gratefully acknowledge NIH support of this work (grant EB002520 to GVN). MIT Lincoln Laboratory funding was not used to support this research.

References

1. Roh JD, Sawh-Martinez R, Brennan MP, Jay SM, Devine L, Rao DA, et al. Tissue-engineered vascular grafts transform into mature blood vessels via an inflammation-mediated process of vascular remodeling. Proc Natl Acad Sci U S A. 2010; 107(10):4669–74. [PubMed: 20207947]
2. Stein M, Keshav S, Harris N, Gordon S. Interleukin 4 potently enhances murine macrophage mannose receptor activity: a marker of alternative immunologic macrophage activation. J Exp Med. 1992; 176(1):287–92. [PubMed: 1613462]
3. Chung ES, Chauhan SK, Jin Y, Nakao S, Hafezi-Moghadam A, van Rooijen N, et al. Contribution of macrophages to angiogenesis induced by vascular endothelial growth factor receptor-3-specific ligands. Am J Pathol. 2009; 175(5):1984–92. [PubMed: 19808642]
4. van Amerongen MJ, Harmsen MC, van Rooijen N, Petersen AH, van Luyn MJ. Macrophage depletion impairs wound healing and increases left ventricular remodeling after myocardial injury in mice. Am J Pathol. 2007; 170(3):818–29. [PubMed: 17322368]
5. Condeelis J, Pollard JW. Macrophages: obligate partners for tumor cell migration, invasion, and metastasis. Cell. 2006; 124(2):263–6. [PubMed: 16439202]
6. Godwin JW, Pinto AR, Rosenthal NA. Macrophages are required for adult salamander limb regeneration. Proc Natl Acad Sci U S A. 2013; 110(23):9415–20. [PubMed: 23690624]
7. Krishnamoorthy, L. MD Thesis. University of Glasgow; 2006. MD thesis: The role of macrophages in human wound healing and their response to a tissue engineered dermal replacement in human chronic wounds.
8. Khallou-Laschet J, Varthaman A, Fornasa G, Compain C, Gaston AT, Clement M, et al. Macrophage plasticity in experimental atherosclerosis. PLoS One. 2010; 5(1):e8852. [PubMed: 20111605]
9. Kigerl KA, Gensel JC, Ankeny DP, Alexander JK, Donnelly DJ, Popovich PG. Identification of two distinct macrophage subsets with divergent effects causing either neurotoxicity or regeneration in the injured mouse spinal cord. J Neurosci. 2009; 29(43):13435–44. [PubMed: 19864556]
10. Lu J, Cao Q, Zheng D, Sun Y, Wang C, Yu X, et al. Discrete functions of M2a and M2c macrophage subsets determine their relative efficacy in treating chronic kidney disease. Kidney Int. 2013; 84(4):745–55. [PubMed: 23636175]
11. Wang Y, Wang YP, Zheng G, Lee VW, Ouyang L, Chang DH, et al. Ex vivo programmed macrophages ameliorate experimental chronic inflammatory renal disease. Kidney Int. 2007; 72(3):290–9. [PubMed: 17440493]
12. Mantovani A, Sozzani S, Locati M, Allavena P, Sica A. Macrophage polarization: tumor-associated macrophages as a paradigm for polarized M2 mononuclear phagocytes. Trends Immunol. 2002; 23(11):549–55. [PubMed: 12401408]
13. Badylak SF, Valentin JE, Ravindra AK, McCabe GP, Stewart-Akers AM. Macrophage phenotype as a determinant of biologic scaffold remodeling. Tissue Eng Part A. 2008; 14(11):1835–42. [PubMed: 18950271]
14. Brown BN, Valentin JE, Stewart-Akers AM, McCabe GP, Badylak SF. Macrophage phenotype and remodeling outcomes in response to biologic scaffolds with and without a cellular component. Biomaterials. 2009; 30(8):1482–91. [PubMed: 19121538]
15. Madden LR, Mortisen DJ, Sussman EM, Dupras SK, Fugate JA, Cuy JL, et al. Proangiogenic scaffolds as functional templates for cardiac tissue engineering. Proc Natl Acad Sci U S A. 2010; 107(34):15211–6. [PubMed: 20696917]
16. Zhang L, Cao Z, Bai T, Carr L, Ella-Menye JR, Irvin C, et al. Zwitterionic hydrogels implanted in mice resist the foreign-body reaction. Nat Biotechnol. 2013; 31(6):553–6. [PubMed: 23666011]

17. Fishman JM, Lowdell MW, Urbani L, Ansari T, Burns AJ, Turmaine M, et al. Immunomodulatory effect of a decellularized skeletal muscle scaffold in a discordant xenotransplantation model. Proc Natl Acad Sci U S A. 2013; 110(35):14360–5. [PubMed: 23940349]
18. Tous E, Weber HM, Lee MH, Koomalsingh KJ, Shuto T, Kondo N, et al. Tunable hydrogel-microsphere composites that modulate local inflammation and collagen bulking. Acta Biomater. 2012; 8(9):3218–27. [PubMed: 22659176]
19. Bota PC, Collie AM, Puolakkainen P, Vernon RB, Sage EH, Ratner BD, et al. Biomaterial topography alters healing in vivo and monocyte/macrophage activation in vitro. J Biomed Mater Res A. 2010; 95(2):649–57. [PubMed: 20725970]
20. Tolg C, Hamilton SR, Zalinska E, McCulloch L, Amin R, Akentieva N, et al. A RHAMM mimetic peptide blocks hyaluronan signaling and reduces inflammation and fibrogenesis in excisional skin wounds. Am J Pathol. 2012; 181(4):1250–70. [PubMed: 22889846]
21. Szekanecz Z, Koch AE. Mechanisms of Disease: angiogenesis in inflammatory diseases. Nat Clin Pract Rheumatol. 2007; 3(11):635–43. [PubMed: 17968334]
22. Cao X, Shen D, Patel MM, Tuo J, Johnson TM, Olsen TW, et al. Macrophage polarization in the maculae of age-related macular degeneration: a pilot study. Pathol Int. 2011; 61(9):528–35. [PubMed: 21884302]
23. Fuentes-Duculan J, Suarez-Farinas M, Zaba LC, Nograles KE, Pierson KC, Mitsui H, et al. A subpopulation of CD163-positive macrophages is classically activated in psoriasis. J Invest Dermatol. 2010; 130(10):2412–22. [PubMed: 20555352]
24. Costa C, Incio J, Soares R. Angiogenesis and chronic inflammation: cause or consequence? Angiogenesis. 2007; 10(3):149–66. [PubMed: 17457680]
25. Peng B, Hao J, Hou S, Wu W, Jiang D, Fu X, et al. Possible pathogenesis of painful intervertebral disc degeneration. Spine (Phila Pa 1976). 2006; 31(5):560–6. [PubMed: 16508552]
26. Hutter R, Speidl WS, Valdiviezo C, Sauter B, Corti R, Fuster V, et al. Macrophages transmit potent proangiogenic effects of oxLDL in vitro and in vivo involving HIF-1alpha activation: a novel aspect of angiogenesis in atherosclerosis. J Cardiovasc Transl Res. 2013; 6(4):558–69. [PubMed: 23661177]
27. Mantovani A, Sica A, Sozzani S, Allavena P, Vecchi A, Locati M. The chemokine system in diverse forms of macrophage activation and polarization. Trends Immunol. 2004; 25(12):677–86. [PubMed: 15530839]
28. Arnold L, Henry A, Poron F, Baba-Amer Y, van Rooijen N, Plonquet A, et al. Inflammatory monocytes recruited after skeletal muscle injury switch into antiinflammatory macrophages to support myogenesis. J Exp Med. 2007; 204(5):1057–69. [PubMed: 17485518]
29. Troidl C, Mollmann H, Nef H, Masseli F, Voss S, Szardien S, et al. Classically and alternatively activated macrophages contribute to tissue remodelling after myocardial infarction. J Cell Mol Med. 2009; 13(9B):3485–96. [PubMed: 19228260]
30. Seager Danciger J, Lutz M, Hama S, Cruz D, Castrillo A, Lazaro J, et al. Method for large scale isolation, culture and cryopreservation of human monocytes suitable for chemotaxis, cellular adhesion assays, macrophage and dendritic cell differentiation. J Immunol Methods. 2004; 288(1–2):123–34. [PubMed: 15183091]
31. Kelley JL, Rozek MM, Suenram CA, Schwartz CJ. Activation of human blood monocytes by adherence to tissue culture plastic surfaces. Exp Mol Pathol. 1987; 46(3):266–78. [PubMed: 3036568]
32. Baudin B, Bruneel A, Bosselut N, Vaubourdolle M. A protocol for isolation and culture of human umbilical vein endothelial cells. Nat Protoc. 2007; 2(3):481–5. [PubMed: 17406610]
33. Preibisch S, Saalfeld S, Tomancak P. Globally optimal stitching of tiled 3D microscopic image acquisitions. Bioinformatics. 2009; 25(11):1463–5. [PubMed: 19346324]
34. Carpentier G. ImageJ Contribution: Angiogenesis analyzer. ImageJ News. 2012:5.
35. Bartneck M, Heffels KH, Pan Y, Bovi M, Zwadlo-Klarwasser G, Groll J. Inducing healing-like human primary macrophage phenotypes by 3D hydrogel coated nanofibres. Biomaterials. 2012; 33(16):4136–46. [PubMed: 22417617]

36. Martinez FO, Gordon S, Locati M, Mantovani A. Transcriptional profiling of the human monocyte-to-macrophage differentiation and polarization: new molecules and patterns of gene expression. J Immunol. 2006; 177(10):7303–11. [PubMed: 17082649]
37. Yoshida A, Anand-Apte B, Zetter BR. Differential endothelial migration and proliferation to basic fibroblast growth factor and vascular endothelial growth factor. Growth Factors. 1996; 13(1–2): 57–64. [PubMed: 8962720]
38. Asahara T, Takahashi T, Masuda H, Kalka C, Chen D, Iwaguro H, et al. VEGF contributes to postnatal neovascularization by mobilizing bone marrow-derived endothelial progenitor cells. EMBO J. 1999; 18(14):3964–72. [PubMed: 10406801]
39. Martin D, Galisteo R, Gutkind JS. CXCL8/IL8 stimulates vascular endothelial growth factor (VEGF) expression and the autocrine activation of VEGFR2 in endothelial cells by activating NFkappaB through the CBM (Carma3/Bcl10/Malt1) complex. J Biol Chem. 2009; 284(10):6038–42. [PubMed: 19112107]
40. Koch AE, Polverini PJ, Kunkel SL, Harlow LA, DiPietro LA, Elner VM, et al. Interleukin-8 as a macrophage-derived mediator of angiogenesis. Science. 1992; 258(5089):1798–801. [PubMed: 1281554]
41. Suffee N, Hlawaty H, Meddahi-Pelle A, Maillard L, Louedec L, Haddad O, et al. RANTES/CCL5-induced pro-angiogenic effects depend on CCR1, CCR5 and glycosaminoglycans. Angiogenesis. 2012; 15(4):727–44. [PubMed: 22752444]
42. Wynn TA, Chawla A, Pollard JW. Macrophage biology in development, homeostasis and disease. Nature. 2013; 496(7446):445–55. [PubMed: 23619691]
43. Sainson RC, Johnston DA, Chu HC, Holderfield MT, Nakatsu MN, Crampton SP, et al. TNF primes endothelial cells for angiogenic sprouting by inducing a tip cell phenotype. Blood. 2008; 111(10):4997–5007. [PubMed: 18337563]
44. Yoshizumi M, Kourembanas S, Temizer DH, Cambria RP, Quertermous T, Lee ME. Tumor necrosis factor increases transcription of the heparin-binding epidermal growth factor-like growth factor gene in vascular endothelial cells. J Biol Chem. 1992; 267(14):9467–9. [PubMed: 1577791]
45. Stratman AN, Schwindt AE, Malotte KM, Davis GE. Endothelial-derived PDGF-BB and HB-EGF coordinately regulate pericyte recruitment during vasculogenic tube assembly and stabilization. Blood. 2010; 116(22):4720–30. [PubMed: 20739660]
46. Hellstrom M, Kalen M, Lindahl P, Abramsson A, Betsholtz C. Role of PDGF-B and PDGFR-beta in recruitment of vascular smooth muscle cells and pericytes during embryonic blood vessel formation in the mouse. Development. 1999; 126(14):3047–55. [PubMed: 10375497]
47. Ponte AL, Marais E, Gallay N, Langonne A, Delorme B, Herault O, et al. The in vitro migration capacity of human bone marrow mesenchymal stem cells: comparison of chemokine and growth factor chemotactic activities. Stem Cells. 2007; 25(7):1737–45. [PubMed: 17395768]
48. Hellberg C, Ostman A, Heldin CH. PDGF and vessel maturation. Recent Results Cancer Res. 2010; 180:103–14. [PubMed: 20033380]
49. Yancopoulos GD, Davis S, Gale NW, Rudge JS, Wiegand SJ, Holash J. Vascular-specific growth factors and blood vessel formation. Nature. 2000; 407(6801):242–8. [PubMed: 11001067]
50. Qi JH, Ebrahem Q, Moore N, Murphy G, Claesson-Welsh L, Bond M, et al. A novel function for tissue inhibitor of metalloproteinases-3 (TIMP3): inhibition of angiogenesis by blockage of VEGF binding to VEGF receptor-2. Nat Med. 2003; 9(4):407–15. [PubMed: 12652295]
51. Rosenberg GA. Matrix metalloproteinases and their multiple roles in neurodegenerative diseases. Lancet Neurol. 2009; 8(2):205–16. [PubMed: 19161911]
52. Jadhav U, Chigurupati S, Lakka SS, Mohanam S. Inhibition of matrix metalloproteinase-9 reduces in vitro invasion and angiogenesis in human microvascular endothelial cells. Int J Oncol. 2004; 25(5):1407–14. [PubMed: 15492832]
53. Ardi VC, Kupriyanova TA, Deryugina EI, Quigley JP. Human neutrophils uniquely release TIMP-free MMP-9 to provide a potent catalytic stimulator of angiogenesis. Proc Natl Acad Sci U S A. 2007; 104(51):20262–7. [PubMed: 18077379]
54. Ebrahem Q, Chaurasia SS, Vasanji A, Qi JH, Klenotic PA, Cutler A, et al. Crosstalk between vascular endothelial growth factor and matrix metalloproteinases in the induction of neovascularization in vivo. Am J Pathol. 2010; 176(1):496–503. [PubMed: 19948826]

55. Fantin A, Vieira JM, Gestri G, Denti L, Schwarz Q, Prykhozhij S, et al. Tissue macrophages act as cellular chaperones for vascular anastomosis downstream of VEGF-mediated endothelial tip cell induction. Blood. 2010; 116(5):829–40. [PubMed: 20404134]
56. Outtz HH, Tattersall IW, Kofler NM, Steinbach N, Kitajewski J. Notch1 controls macrophage recruitment and Notch signaling is activated at sites of endothelial cell anastomosis during retinal angiogenesis in mice. Blood. 2011; 118(12):3436–9. [PubMed: 21795743]
57. Ju YM, Yu B, West L, Moussy Y, Moussy F. A novel porous collagen scaffold around an implantable biosensor for improving biocompatibility. II. Long-term in vitro/in vivo sensitivity characteristics of sensors with NDGA- or GA-crosslinked collagen scaffolds. J Biomed Mater Res A. 2010; 92(2):650–8. [PubMed: 19235209]
58. Mao Z, Shi H, Guo R, Ma L, Gao C, Han C, et al. Enhanced angiogenesis of porous collagen scaffolds by incorporation of TMC/DNA complexes encoding vascular endothelial growth factor. Acta Biomater. 2009; 5(8):2983–94. [PubMed: 19406694]
59. Stevens KR, Einerson NJ, Burmania JA, Kao WJ. In vivo biocompatibility of gelatin-based hydrogels and interpenetrating networks. J Biomater Sci Polym Ed. 2002; 13(12):1353–66. [PubMed: 12555901]
60. Kitajewski J. Wnts heal by restraining angiogenesis. Blood. 2013; 121(13):2381–2. [PubMed: 23538232]
61. Kiriakidis S, Andreakos E, Monaco C, Foxwell B, Feldmann M, Paleolog E. VEGF expression in human macrophages is NF-kappaB-dependent: studies using adenoviruses expressing the endogenous NF-kappaB inhibitor IkappaBalpha and a kinase-defective form of the IkappaB kinase 2. J Cell Sci. 2003; 116(Pt 4):665–74. [PubMed: 12538767]
62. Takeda Y, Costa S, Delamarre E, Roncal C, Leite de Oliveira R, Squadrito ML, et al. Macrophage skewing by Phd2 haplodeficiency prevents ischaemia by inducing arteriogenesis. Nature. 2011; 479(7371):122–6. [PubMed: 21983962]
63. Anders HJ, Ryu M. Renal microenvironments and macrophage phenotypes determine progression or resolution of renal inflammation and fibrosis. Kidney Int. 2011; 80(9):915–25. [PubMed: 21814171]
64. Matull WR, Dhar DK, Ayaru L, Sandanayake NS, Chapman MH, Dias A, et al. R0 but not R1/R2 resection is associated with better survival than palliative photodynamic therapy in biliary tract cancer. Liver Int. 2011; 31(1):99–107. [PubMed: 20846273]
65. Pereira TA, Xie G, Choi SS, Syn WK, Voieta I, Lu J, et al. Macrophage-derived Hedgehog ligands promotes fibrogenic and angiogenic responses in human schistosomiasis mansoni. Liver Int. 2013; 33(1):149–61. [PubMed: 23121638]
66. Franz S, Rammelt S, Scharnweber D, Simon JC. Immune responses to implants - a review of the implications for the design of immunomodulatory biomaterials. Biomaterials. 2011; 32(28):6692–709. [PubMed: 21715002]
67. Murray PJ, Wynn TA. Protective and pathogenic functions of macrophage subsets. Nat Rev Immunol. 2011; 11(11):723–37. [PubMed: 21997792]
68. Low-Marchelli JM, Ardi VC, Vizcarra EA, van Rooijen N, Quigley JP, Yang J. Twist1 induces CCL2 and recruits macrophages to promote angiogenesis. Cancer Res. 2013; 73(2):662–71. [PubMed: 23329645]
69. Kubota Y, Takubo K, Shimizu T, Ohno H, Kishi K, Shibuya M, et al. M-CSF inhibition selectively targets pathological angiogenesis and lymphangiogenesis. J Exp Med. 2009; 206(5):1089–102. [PubMed: 19398755]
70. Arendt LM, McCready J, Keller PJ, Baker DD, Naber SP, Seewaldt V, et al. Obesity Promotes Breast Cancer by CCL2-Mediated Macrophage Recruitment and Angiogenesis. Cancer Res. 2013; 73(19):6080–93. [PubMed: 23959857]
71. Sakurai E, Anand A, Ambati BK, van Rooijen N, Ambati J. Macrophage depletion inhibits experimental choroidal neovascularization. Invest Ophthalmol Vis Sci. 2003; 44(8):3578–85. [PubMed: 12882810]
72. Hibino N, Yi T, Duncan DR, Rathore A, Dean E, Naito Y, et al. A critical role for macrophages in neovessel formation and the development of stenosis in tissue-engineered vascular grafts. FASEB J. 2011; 25(12):4253–63. [PubMed: 21865316]

73. Hisatome T, Yasunaga Y, Yanada S, Tabata Y, Ikada Y, Ochi M. Neovascularization and bone regeneration by implantation of autologous bone marrow mononuclear cells. Biomaterials. 2005; 26(22):4550–6. [PubMed: 15722124]
74. Hirose N, Maeda H, Yamamoto M, Hayashi Y, Lee GH, Chen L, et al. The local injection of peritoneal macrophages induces neovascularization in rat ischemic hind limb muscles. Cell Transplant. 2008; 17(1–2):211–22. [PubMed: 18468252]
75. Herbert SP, Stainier DY. Molecular control of endothelial cell behaviour during blood vessel morphogenesis. Nat Rev Mol Cell Biol. 2011; 12(9):551–64. [PubMed: 21860391]
76. He H, Xu J, Warren CM, Duan D, Li X, Wu L, et al. Endothelial cells provide an instructive niche for the differentiation and functional polarization of M2-like macrophages. Blood. 2012; 120(15): 3152–62. [PubMed: 22919031]
77. Eirin A, Zhu XY, Li Z, Ebrahimi B, Zhang X, Tang H, et al. Endothelial outgrowth cells shift macrophage phenotype and improve kidney viability in swine renal artery stenosis. Arterioscler Thromb Vasc Biol. 2013; 33(5):1006–13. [PubMed: 23430615]
78. Baer C, Squadrito ML, Iruela-Arispe ML, De Palma M. Reciprocal interactions between endothelial cells and macrophages in angiogenic vascular niches. Exp Cell Res. 2013
79. Agrawal H, Tholpady SS, Capito AE, Drake DB, Katz AJ. Macrophage phenotypes correspond with remodeling outcomes of various acellular dermal matrices. Open Journal of Regenerative Medicine. 2012; 1(3):51–9.
80. Anderson, JM. In vitro and in vivo monocyte, macrophage, foreign body giant cell, and lymphocyte interactions with biomaterials. In: Puleo, DA.; Bizios, R., editors. Biological Interactions on Materials Surfaces. Springer Science + Business Media; 2009. p. 225-45.
81. Kao WJ, McNally AK, Hiltner A, Anderson JM. Role for interleukin-4 in foreign-body giant cell formation on a poly(etherurethane urea) in vivo. J Biomed Mater Res. 1995; 29(10):1267–75. [PubMed: 8557729]
82. McNally AK, DeFife KM, Anderson JM. Interleukin-4-induced macrophage fusion is prevented by inhibitors of mannose receptor activity. Am J Pathol. 1996; 149(3):975–85. [PubMed: 8780401]
83. Lolmede K, Campana L, Vezzoli M, Bosurgi L, Tonlorenzi R, Clementi E, et al. Inflammatory and alternatively activated human macrophages attract vessel-associated stem cells, relying on separate HMGB1- and MMP-9-dependent pathways. J Leukoc Biol. 2009; 85(5):779–87. [PubMed: 19197071]
84. Zizzo G, Hilliard BA, Monestier M, Cohen PL. Efficient clearance of early apoptotic cells by human macrophages requires M2c polarization and MerTK induction. J Immunol. 2012; 189(7): 3508–20. [PubMed: 22942426]
85. Spiller KL, Vunjak-Novakovic G. Clinical translation of controlled protein delivery systems for tissue engineering. Drug Deliv and Transl Res. 2013
86. Seok J, Warren HS, Cuenca AG, Mindrinos MN, Baker HV, Xu W, et al. Genomic responses in mouse models poorly mimic human inflammatory diseases. Proc Natl Acad Sci U S A. 2013; 110(9):3507–12. [PubMed: 23401516]

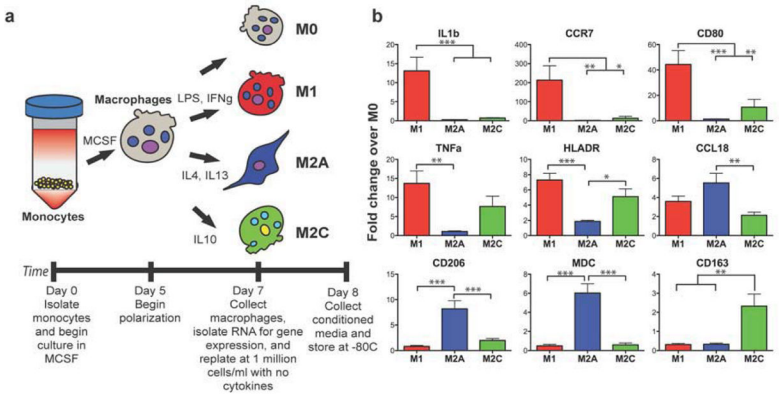

Figure 1. Derivation and characteristics of macrophages

(a) Peripheral blood monocytes were differentiated to macrophages (M0) and polarized to 3 different phenotypes (M1, M2a, M2c). **(b)** Gene expression of some known markers of macrophage phenotype (RT-PCR using monocytes/macrophages from n = 9 human donors). Data are shown as Mean ± SEM. $^{*}p<0.05$, $^{**}p<0.01$, $^{***}p<0.001$.

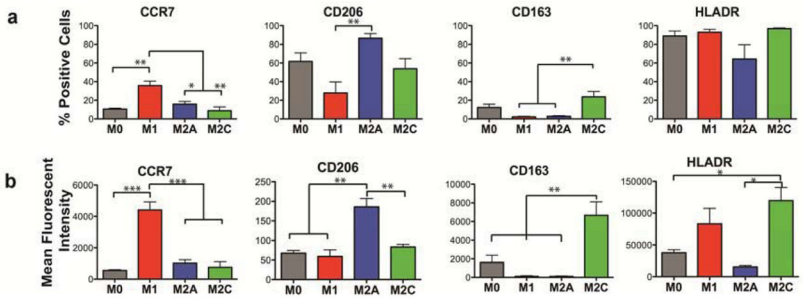

Figure 2. Flow cytometric analysis of macrophage phenotype markers

(a) The percentage of cells staining positively for the surface marker, and **(b)** mean fluorescent intensity per cell (n = 3–5 human donors). Data are shown as Mean ± SEM. $^{*}p<0.05$, $^{**}p<0.01$, $^{***}p<0.001$.

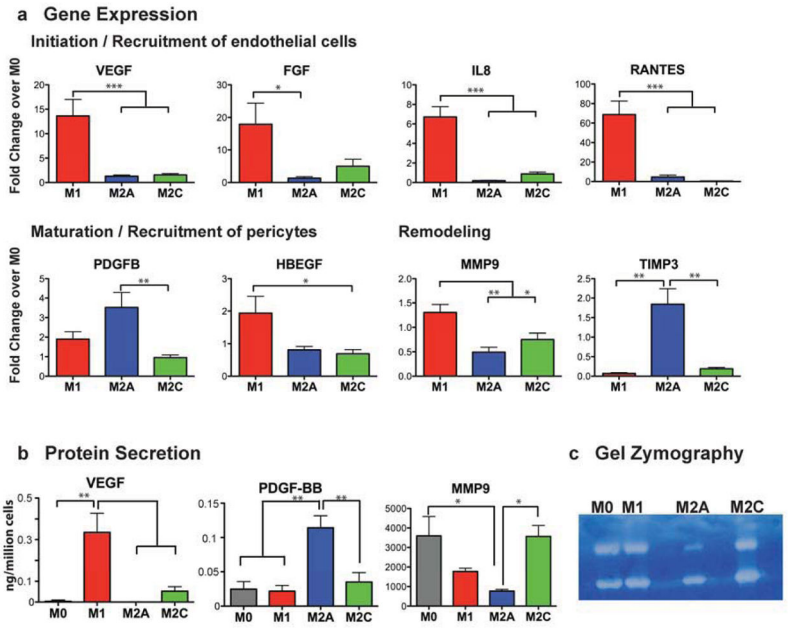

Figure 3. Gene expression and protein secretion levels of different macrophage phenotypes

(a) Gene expression of proteins typically associated with the initiation of angiogenesis (VEGF, FGF, IL8, RANTES), the maturation of growing blood vessels (PDGFBB, HBEGF), and remodeling of the vascular network (MMP9, TIMP3) (RT-PCR using monocytes/macrophages from n = 9 human donors). **(b)** ELISA of macrophage-conditioned media for levels of protein secretion (n = 4–6 human donors). **(c)** Enzymatic activity for MMP-9 was confirmed by gel zymography (representative gel shown, n = 5 human donors). Data are presented as Mean ± SEM. $^{*}p<0.05$, $^{**}p<0.01$, $^{***}p<0.001$.

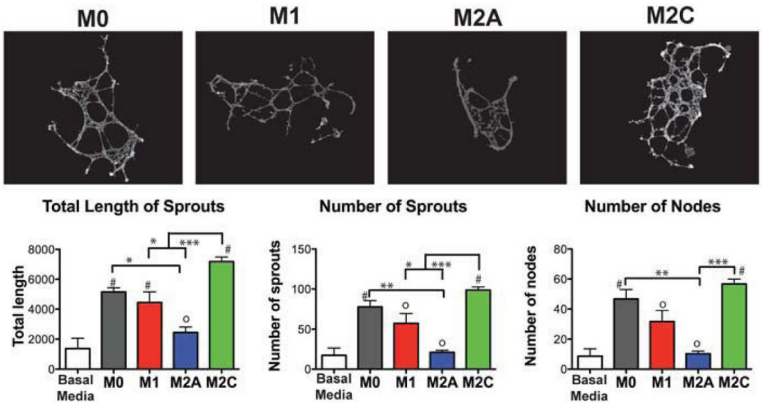

Figure 4. Functionality of macrophage-secreted factors in angiogenesis in vitro

An *in vitro* sprouting assay was used to assess HUVEC organization on Matrigel® in macrophage-conditioned media. Networks were analyzed using the Angiogenesis Analyzer macro in ImageJ following background subtraction in MATLAB. Data are shown as Mean ± SEM (3–5). ^{0}Non-significant differences compared to control group (Basal media only); $^{\#}$Significantly different from control group. $^{*}p<0.05$, $^{**}p<0.01$, $^{***}p<0.001$.

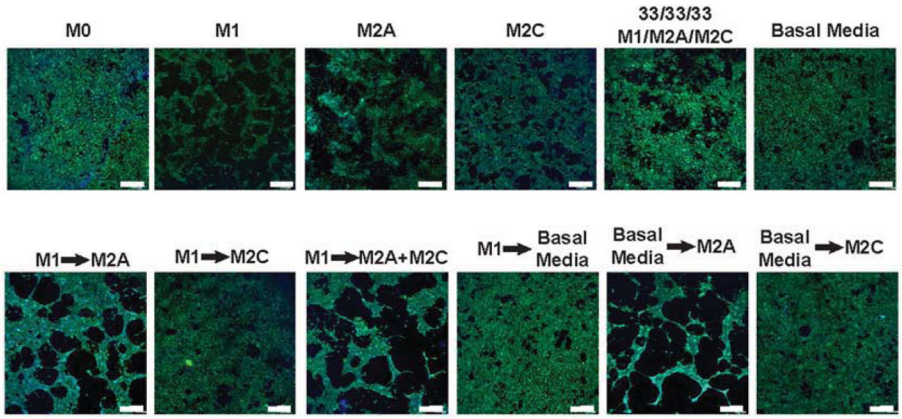

Figure 5. Organization of HUVECs on fibrin gel when cultured in macrophage-conditioned media for 4 days

The behavior of endothelial cells in media conditioned by a single macrophage phenotype was compared to that of endothelial cells cultured in media that was switched after 24hrs from one macrophage phenotype to another. Cell nuclei were stained with DAPI (blue) and actin filaments were stained with fluorescent phalloidin (green). Experiments were repeated three times. Scale bars are 500μm.

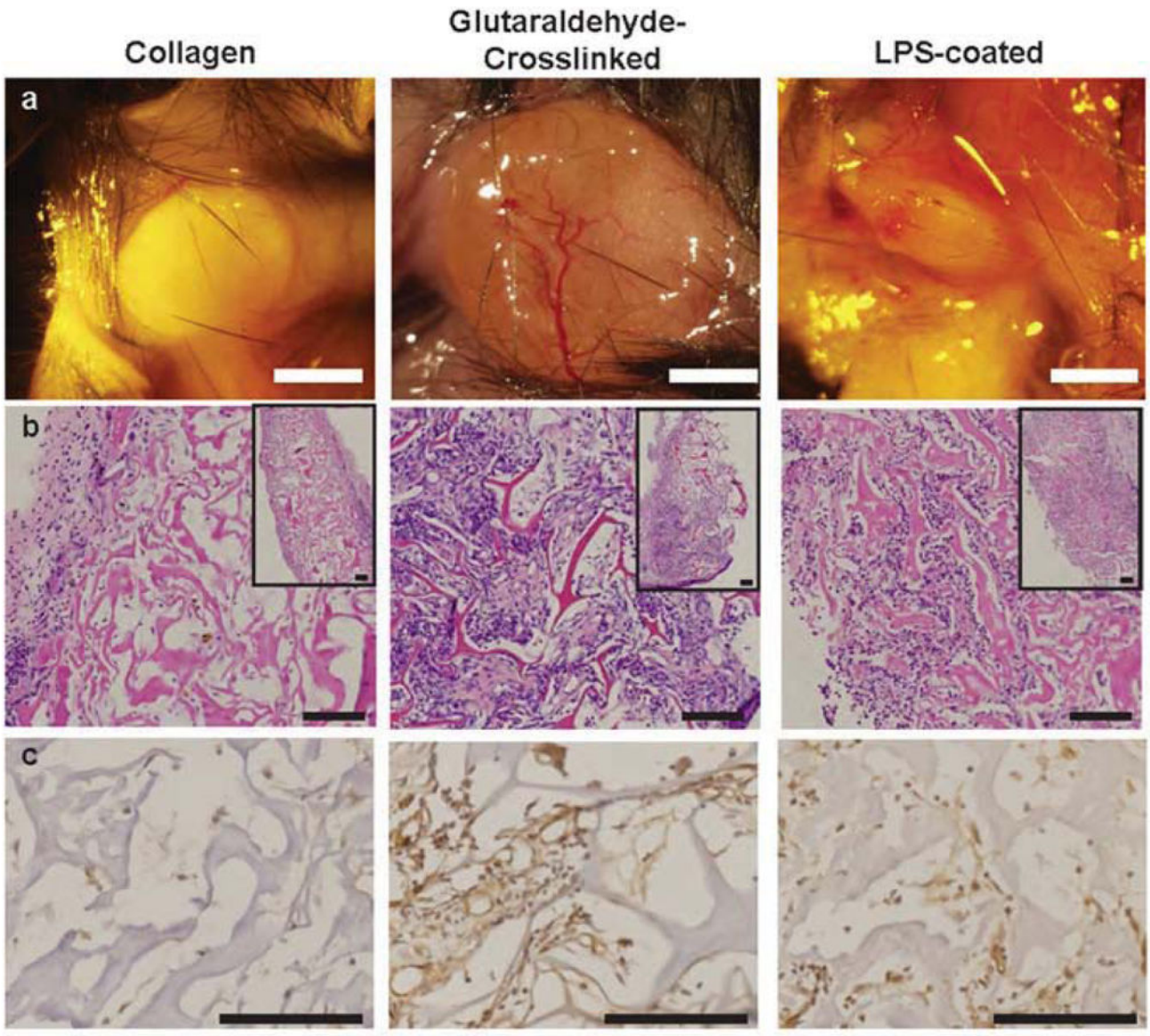

Figure 6. Relationships between macrophage phenotype and scaffold vascularization *in vivo* after 10 days in a subcutaneous implantation model in mice

(a) Gross view of scaffolds upon explantation. Scale bar is 2mm. **(b)** H&E staining. Scale bars are 100μm. **(c)** Immunohistochemical staining for the endothelial cell marker CD31. Scale bars are 100μm. Representative images are shown from n= 4–6 replicates.

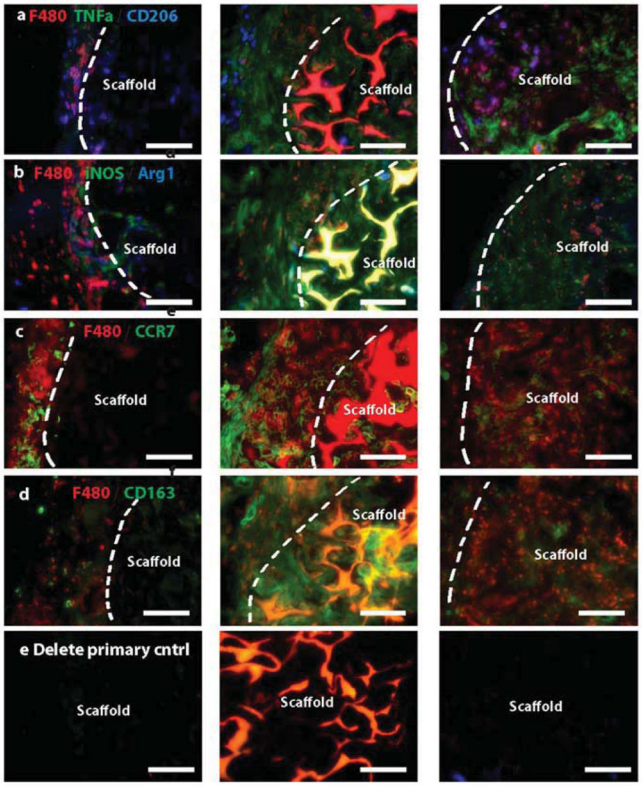

Figure 7. Immunohistochemical analysis of macrophage phenotype markers

Sections of explanted scaffolds with surrounding tissue were stained for multiple markers of M1 and M2 macrophage phenotypes in combination with the pan-macrophage marker F480. M1 markers are TNFa (a), iNOS (b), and CCR7 (c). M2 markers are CD206 (a), Arg1 (b), and CD163 (d). Scale bars are 100μm. Representative images are shown from n= 4–6 replicates. (e) Delete primary controls. Glutaraldehyde-crosslinked exhibited substantial autofluorescence.

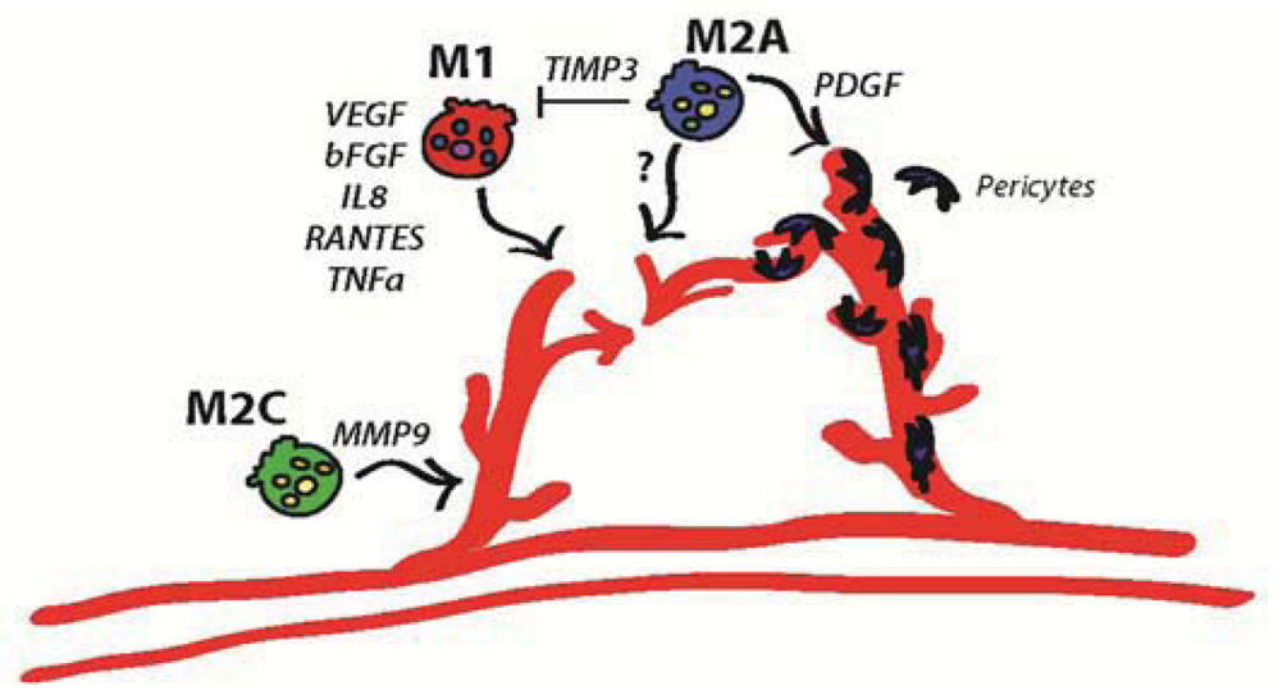

Figure 8. Proposed model of macrophage-mediated angiogenesis

M1 macrophages promote sprouting of blood vessels via secretion of VEGF, bFGF, IL8, RANTES, and TNFa. M2a macrophages promote fusion of blood vessels through as-yet unidentified secreted factors. M2a macrophages may also regulate the actions of M1 macrophages via production of TIMP3, and may recruit pericytes via secretion of PDGF-BB, although this was not directly assessed in this study. M2c macrophages may function in vascular remodeling, given their high levels of production of MMP9.

Table 1

Qualitative observations for immunofluorescent staining of macrophage phenotype in explanted scaffolds and surrounding tissue from *in vivo* study (Fig. 7a–d).

Marker	Collagen	Glutaraldehyde-Crosslinked	LPS-coated
TNFa (M1)	+	+++	+++
iNOS (M1)	+	+++	++
CCR7 (M1)	++	++	++
CD206 (M2)	++	++	++
Arg1 (M2)	+++	–	+
CD163 (M2)	++	+++	+